Demonstration of Controlled-Phase Gates between Two Error-Correctable Photonic Qubits

Y. Xu,[1,*] Y. Ma,[1,*] W. Cai,[1] X. Mu,[1] W. Dai,[1] W. Wang,[1] L. Hu,[1] X. Li,[1] J. Han,[1] H. Wang,[1] Y. P. Song,[1] Zhen-Biao Yang,[2,†] Shi-Biao Zheng,[2,‡] and L. Sun[1,§]

[1]*Center for Quantum Information, Institute for Interdisciplinary Information Sciences, Tsinghua University, Beijing 100084, China*
[2]*Fujian Key Laboratory of Quantum Information and Quantum Optics, College of Physics and Information Engineering, Fuzhou University, Fuzhou, Fujian 350108, China*

(Received 10 October 2018; revised manuscript received 9 October 2019; accepted 28 February 2020; published 24 March 2020)

To realize fault-tolerant quantum computing, it is necessary to store quantum information in logical qubits with error correction functions, realized by distributing a logical state among multiple physical qubits or by encoding it in the Hilbert space of a high-dimensional system. Quantum gate operations between these error-correctable logical qubits, which are essential for implementation of any practical quantum computational task, have not been experimentally demonstrated yet. Here we demonstrate a geometric method for realizing controlled-phase gates between two logical qubits encoded in photonic fields stored in cavities. The gates are realized by dispersively coupling an ancillary superconducting qubit to these cavities and driving it to make a cyclic evolution depending on the joint photonic state of the cavities, which produces a conditional geometric phase. We first realize phase gates for photonic qubits with the logical basis states encoded in two quasiorthogonal coherent states, which have important implications for continuous-variable-based quantum computation. Then we use this geometric method to implement a controlled-phase gate between two binomially encoded logical qubits, which have an error-correctable function.

DOI: 10.1103/PhysRevLett.124.120501

Quantum computers process information in a way fundamentally different from their classical counterparts, where information is encoded in the state of a collection of quantum bits (qubits) and algorithms are carried out by performing a sequence of gates on these qubits [1]. Unlike classical bits, qubits are vulnerable to decoherence arising from coupling to the environment and noises of the control fields, which is one of the main obstacles to construct a large-scale quantum computer. To make a quantum computer function under decoherence effects, quantum information has to be stored in logical qubits, with which errors can be detected and corrected. In traditional quantum error correction (QEC) schemes, a logical qubit is redundantly encoded in multiple physical qubits [2]. QEC based on these kinds of encoding schemes has been demonstrated in various systems, including nuclear spins [3,4], nitrogen-vacancy centers in diamond [5–7], photons [8], trapped ions [9–11], and superconducting qubits [12–16]. To run a quantum algorithm with these logical qubits, it is necessary to be capable of performing quantum gate operations between them, but which have not been demonstrated yet.

Error-correctable logical qubits can also be constructed by encoding the quantum information in the large Hilbert space of a harmonic oscillator, whose state can be controlled by using an ancillary qubit resonantly [17–19] or dispersively [20–24] coupled to it. The Schrödinger cat code [25,26] and the binomial code [27] are paradigms of this approach, with each of which demonstrations of QEC have been reported in superconducting circuits [28,29], where an ancillary transmon qubit dispersively coupled to a three-dimensional cavity is used to detect and correct the photon loss of the multiphoton logical qubit stored in the cavity. With similar setups, universal single-qubit gate sets based on both encodings were realized by the gradient ascent pulse engineering (GRAPE) method [29,30]. Recently, a quantum controlled-NOT gate between two asymmetrically encoded photonic qubits, respectively, stored in two cavities has been demonstrated [31]. This gate was realized by encoding the codewords of the control qubit on the vacuum state and two-photon state, which form a logical space where errors due to photon loss cannot be corrected. Entangling gate operations between two error-correctable logical qubits still remain elusive.

We here demonstrate a geometric method which enables realization of controlled-phase gates for photonic qubits with different encodings, in particular for two error-correctable logical qubits by using an ancillary transmon qubit dispersively coupled to the cavities storing the corresponding photonic qubits. With two successive carefully designed microwave pulses, the ancillary qubit is parallel transported along a closed loop on the Bloch sphere, picking up a geometric phase [32–37], conditional on the particular component of the photonic qubits. The magnitude of the acquired geometric phase is controllable

by the phase difference between the two applied pulses. We first employ this geometric phase to realize single- and two-cavity phase gates with coherent-state encoding. With this encoding, the single-cavity phase gate corresponds to manipulating the photon-number parity of a multiphotonic cat state. We further extend our method to implement a controlled-Z (CZ) gate between two binomial logical qubits, each of which has inherent error correction function. We demonstrate that this gate can evolve the two logical qubits to a maximally entangled state. The procedure can be straightforwardly and easily generalized to realize phase gates among multiple error-correctable logical qubits.

The experiments presented in this work are based on two circuit quantum electrodynamics (QED) devices [38–42]. Device A, on which single-cavity geometric phase gates are performed, consists of two transmon qubits simultaneously dispersively coupled to two three-dimensional cavities [43–45]. The parameters and architecture setup are described in Ref. [46]. Device B, on which two-cavity geometric phase gates are performed, consists of three transmon qubits dispersively coupled to two cylindrical cavities [47] and three stripline readout cavities [48]. The device parameters are described in Ref. [49]. In device A, the coupling between the qubit (Q_1) used to produce the geometric phase and the cavity used to encode this phase is described by the Hamiltonian

$$H = -\hbar\chi_{\rm qs} a^\dagger a|e\rangle\langle e|, \tag{1}$$

where $\chi_{\rm qs}$ denotes the qubit frequency shift induced by per photon, $a^\dagger$ and a are the creation and annihilation operators for the particular cavity field, respectively, and $|e\rangle$ ($|g\rangle$) is the excited (ground) state of the qubit. In device B, the qubit, commonly coupled to two cavities used to store the photonic qubits, undergoes a frequency shift dependent on the photon numbers of both cavities.

The geometric manipulation technique is well exemplified with the even cat state $(|\alpha\rangle_c + |-\alpha\rangle_c)/\sqrt{2}$, where $|\alpha\rangle_c$ and $|-\alpha\rangle_c$ are coherent states, which can act as the two basis states of a logical qubit when ${}_c\langle\alpha|-\alpha\rangle_c \approx O(e^{-2|\alpha|^2}) \ll 1$. To realize conditional qubit rotations, a phase-space displacement, $D(\alpha)$, is applied to the cavity, transforming its state to $(|2\alpha\rangle_c + |0\rangle)/\sqrt{2}$. The qubit, initially in the ground state $|g\rangle$, is then driven by a classical field on resonance with the qubit frequency conditioned on the cavity's vacuum state $|0\rangle$. We here assume that the Rabi frequency ε of the drive is much smaller than $\bar{n}\chi_{\rm qs}$, where $\bar{n} = 4|\alpha|^2$ is the average photon number of the state $|2\alpha\rangle_c$. In this case, the qubit's state is not changed by the drive when the cavity is in $|2\alpha\rangle_c$ due to the large detuning, and the system dynamics is described by the effective Hamiltonian

$$H_{\rm eff} = \frac{1}{2}\hbar\epsilon e^{i\phi}|e\rangle\langle g| \otimes |0\rangle\langle 0| + \text{H.c.}, \tag{2}$$

where ϕ is the phase of the drive. This Hamiltonian produces a qubit rotation $R^\theta_{\mathbf{n}}$ conditional on the cavity's vacuum state, where $R^\theta_{\mathbf{n}}$ represents the operation that rotates the qubit's state by an angle $\theta = \int_0^\tau \varepsilon dt$ around the axis $\mathbf{n}$ with an angle ϕ to x axis on the equatorial plane of the Bloch sphere, with τ being the pulse duration.

After two successive conditional π rotations $R^{\pi,0}_{\mathbf{n}_1} = R^\pi_{\mathbf{n}_1} \otimes |0\rangle\langle 0|$ and $R^{\pi,0}_{\mathbf{n}_2} = R^\pi_{\mathbf{n}_2} \otimes |0\rangle\langle 0|$, the qubit makes a cyclic evolution, returning to the initial state $|g\rangle$ but acquiring a phase $\gamma = \pi + \Delta\phi = \Omega/2$, where $\Delta\phi = \phi_1 - \phi_2$ represents the angle between the two rotation axes, and Ω is the solid angle subtended by the trajectory traversed by the qubit on the Bloch sphere, as shown in Fig. 1(a). This conditional phase shift leads to the cavity state $(|2\alpha\rangle_c + e^{i\gamma}|0\rangle)/\sqrt{2}$. A subsequent displacement $D(-\alpha)$ transforms the cavity to the state $(|\alpha\rangle_c + e^{i\gamma}|-\alpha\rangle_c)/\sqrt{2}$, realizing the phase gate. Because of the quantum interference of the two superposed coherent state components $|\alpha\rangle_c$ and $|-\alpha\rangle_c$, the cavity photon-number parity P exhibits a periodical oscillation when the geometric phase γ is varied: $P = \cos\gamma$. This procedure allows for manipulation of the parity of the cat state; when $\gamma = \pi$, the parity is reversed.

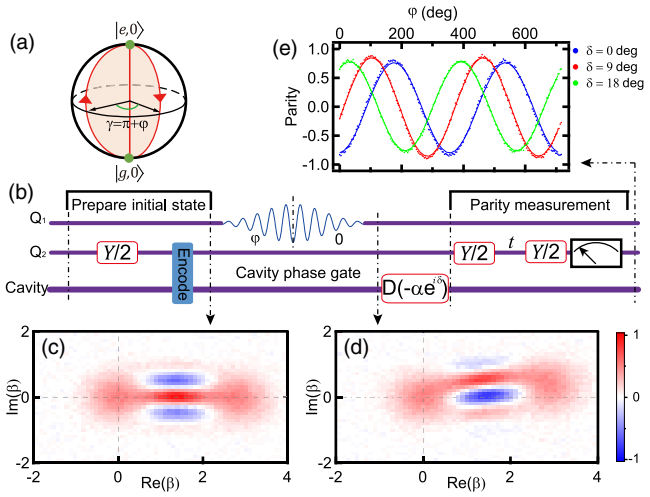

FIG. 1. Geometric manipulation of a photonic cat state. (a) Schematic of the nonadiabatic AA phase of a qubit. Two successive π rotations of the qubit produce a geometric phase $\gamma = \pi + \varphi$, where φ is the angle between the two rotation axes. (b) Experimental sequence to manipulate the cat state. A cavity is dispersively coupled to the qubit and initialized in a cat state $(|0\rangle + |2\alpha\rangle_c)/\sqrt{2}$ with the help of an ancillary qubit Q_2. The AA phase produced by the rotations of Q_1 conditional on the cavity's vacuum state is encoded in the probability amplitude of $|0\rangle$, resulting in a phase gate. (c) Measured Wigner function of the cavity state before the phase gate, corresponding to fidelity of 0.980 to the ideal cat state. (d) Wigner function of the cavity state after the gate with $\varphi = 0$. The slight rotation and deformation of the Wigner function is due to the self-Kerr effect of the cavity. (e) Measured parity of the cavity state as a function of φ after a displacement $D(-\alpha e^{i\delta})$ for different values of δ. Symbols are experimental data, in excellent agreement with numerical simulations (solid lines).

To simplify the operation, in our experiment the cavity displacement before the conditional qubit rotation is incorporated with the preparation of the initial cavity state; $|2\alpha\rangle_c$ and $|0\rangle$ instead act as the two logical basis states $|0\rangle_L$ and $|1\rangle_L$ for the single-cavity phase gate demonstration. We note that there is a compromise of choosing the value of α. On one hand, a larger cat size is favorite for decreasing the overlapping between the two coherent state components, and for shortening the gate duration. On the other hand, the gate infidelity caused by the Kerr effects increases with the cat size. In our experiment, $\alpha = \sqrt{2}$; with this setting the total gate error is minimized. The experimental sequence to manipulate a cat state with device A is shown in Fig. 1(b). The cavity is initialized in the cat state $(|2\alpha\rangle_c + |0\rangle)/\sqrt{2}$ [the measured Wigner function is shown in Fig. 1(c)] with the help of ancillary qubit Q_2 following the GRAPE technique [50,51]. The two subsequent conditional π rotations on Q_1 yield a geometric phase $\gamma = \pi + \varphi$ conditional on $|0\rangle$, where φ is the angle between the two rotation axes. The Wigner function of the cavity state after this single-cavity geometric phase gate is shown in Fig. 1(d) with $\varphi = 0$. After a displacement $D(-\alpha e^{i\delta})$, the parity of the cavity state as a function of φ is measured and shown in Fig. 1(e), in excellent agreement with numerical simulations.

Quantum process tomography (QPT) is used to benchmark the cavity geometric phase gate performance, with the experimental sequence shown in Fig. 2(a). Since trusted operations and measurements necessary for QPT are unavailable in the coherent-state-encoded subspace, we characterize the gate by decoding the quantum information on the cavity back to the transmon qubit Q_2. We use the so-called Pauli transfer process R matrix as a measure of our gate [52], which connects the input and output Pauli operators with $P_{\text{out}} = RP_{\text{in}}$. Figure 2(b) shows the R matrix fidelity decay as a function of m, the number of the π phase (Z) gate. The fidelity at $m = 0$ quantifies the "round trip" process fidelity $F_{\text{ED}} = 0.969$ of the encoding and decoding processes only. A linear fit of the process fidelity decay gives the Z gate fidelity $F_Z = 0.987$, also consistent with the fidelity calculated from $F_Z = 1 - (F_{\text{ED}} - F_{Z\_\text{ED}})$, where $F_{Z\_\text{ED}} = 0.957$ is the measured fidelity including the encoding and decoding processes. The measured and the ideal Pauli transfer R matrices of the S gate and T gate are shown in Fig. 2(c), where $S = |0\rangle_L\langle 0| + i|1\rangle_L\langle 1|$ and $T = |0\rangle_L\langle 0| + \exp(i\pi/4)|1\rangle_L\langle 1|$.

Our method can be directly generalized to implementation of controlled-phase gates between two photonic qubits encoded in two cavities that are dispersively coupled to one common superconducting qubit [53,54]. Figure 3 shows the two-cavity geometric phase gates based on device B, whose schematic is shown in Fig. 3(a). Besides the transmon qubit commonly connected to both cavities, each cavity is individually coupled to another ancillary transmon qubit for encoding and decoding and measurement

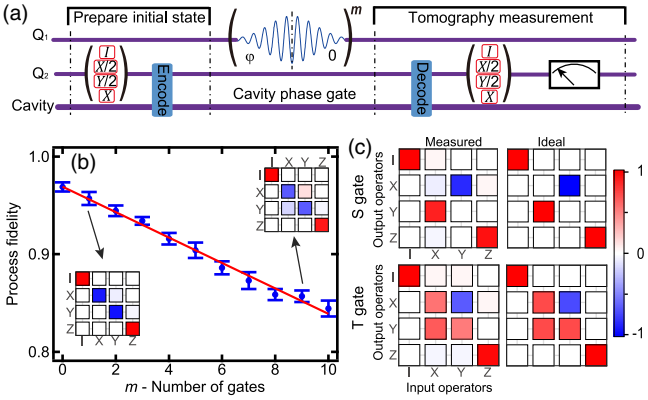

FIG. 2. Quantum process tomography (QPT) of single-cavity geometric phase gates. (a) Experimental sequence. (b) The Pauli transfer process R matrix fidelity as a function of m, the number of the Z gate on the cavity state. The insets show the measured R matrices after one and nine Z gates, respectively. A linear fit of the process fidelity decay gives the Z gate fidelity $F_Z = 0.987 \pm 0.001$. (c) The measured and ideal Pauli transfer R matrices of the S gate and T gate with fidelities $F_S = 0.968$ and $F_T = 0.964$.

purposes. A two-cavity CZ gate with the coherent state encoding $\{|0\rangle_L = |\alpha\rangle_c, |1\rangle_L = |-\alpha\rangle_c\}$ for both cavities is implemented by sandwiching a conditional qubit rotation between two pairs of displacement operations. The first pair of displacements transform the coherent states $|\alpha\rangle_c$ and $|-\alpha\rangle_c$ of each cavity to $|2\alpha\rangle_c$ and $|0\rangle$, respectively. The subsequent pulse, applied to the common qubit, produces a 2π rotation conditional on each cavity being in the vacuum state. The second pair of displacements restore each coherent state to the original amplitude. Consequently, the two cavities undergo a π phase shift if and only if they are both in the logical state $|1\rangle_L$.

Here, we use the two-cavity QPT method to benchmark the performance of our realized CZ gate, with the experimental sequence shown in Fig. 3(b). We first prepare the two cavities in a product state $|0\rangle_L(|0\rangle_L + |1\rangle_L)/\sqrt{2}$ or $|1\rangle_L(|0\rangle_L + |1\rangle_L)/\sqrt{2}$ in two separate experiments. After performing the two-cavity CZ gate, the even cat state $(|\alpha\rangle_c + |-\alpha\rangle_c)/\sqrt{2}$ in the target cavity S_1 evolves to even (odd) cat state when the control cavity S_2 prepared in $|0\rangle_L$ ($|1\rangle_L$), which is verified by the Wigner functions of the target cavity S_1 measured before and after the two-cavity CZ gate as shown in Fig 3(c).

With the two-cavity QPT method, we fully characterize the realized CZ gate with the measured Pauli transfer R matrix, together with that for the ideal CZ gate, displaced in Fig. 3(d). The obtained process R matrix fidelities, $F_{\text{CZ\_ED}}$ and F_{ED}, are respectively 0.859 and 0.954, which indicate the intrinsic two-cavity CZ gate fidelity is $F_{\text{CZ}} = 0.905$, with the infidelities mainly coming from the control pulse imperfections [49].

Our method allows implementation of a gate between two error-correctable logical qubits. For logical qubits

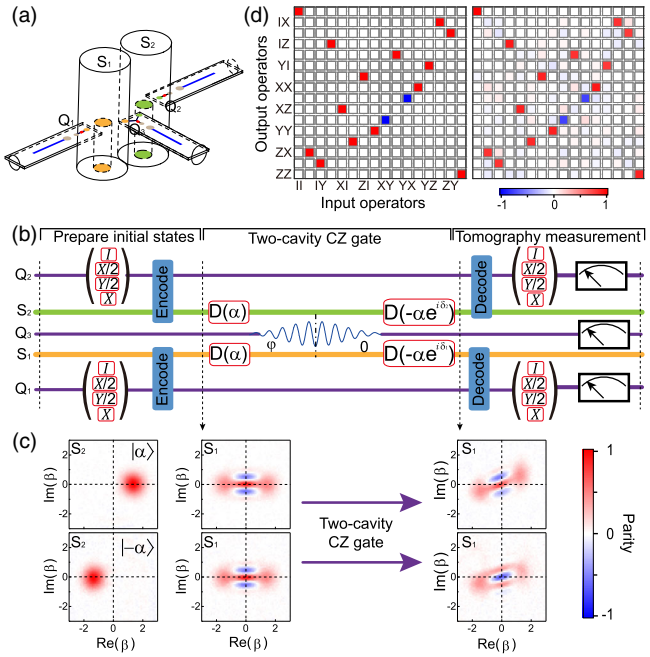

FIG. 3. Two-cavity geometric phase gate. (a) A 3D view of device B. A superconducting transmon qubit Q_3 at the center couples to two coaxial cavities S_1 and S_2, which couple to two other individual ancillary transmon qubits Q_1 and Q_2, respectively. Each of these transmon qubits independently couples to a stripline readout resonator used to perform simultaneous single-shot readout. (b) Schematic of the experimental sequence. (c) Measured individual Wigner functions of storage cavity S_1 and S_2. When the control cavity S_2 prepared in $|\alpha\rangle_c$ ($|-\alpha\rangle_c$), the even cat state $(|\alpha\rangle_c + |-\alpha\rangle_c)/\sqrt{2}$ in target cavity S_1 evolves to even (odd) cat state under the two-cavity CZ gate. The slight rotation and deformation of the Wigner functions after gate are due to the Kerr effect of the cavities. (d) Ideal (left) and measured (right) Pauli transfer R matrices of the two-cavity CZ gate with the coherent encoding $\{|0\rangle_L = |\alpha\rangle_c, |1\rangle_L = |-\alpha\rangle_c\}$. The corresponding process fidelity $F_{\mathrm{CZ\_ED}}$ (F_{ED}) is 0.859 (0.954).

whose basis states are encoded in even cat states, the photon-number parity can be used as an error syndrome of the single-photon loss [25,26,28,64]. With this encoding, each of the two-qubit logical basis states is composed of four two-mode coherent state components, and a CZ gate can be realized by subsequently performing four conditional phase operations. We note that the displacements necessary for realizing these operations will move the logical qubits out of the error-correctable logical space. This problem can be overcome with another kind of error-correctable logical qubits binomially encoded as $\{|0\rangle_L = (|0\rangle + |4\rangle_F)/\sqrt{2}, |1\rangle_L = |2\rangle_F\}$ [27,29].

To demonstrate the applicability of our method to binomial logical qubits, we first binomially encode the two cavities, then perform a CZ gate between thus-encoded qubits via geometric manipulation, and finally read out their joint state. The experimental sequence is similar to that in Fig. 3(b) but without the displacements. Because of the limitation of the dispersive couplings between the ancillary qubit and the cavities, the drive tuned to the ancilla's frequency associated with the cavities' basis state $|22\rangle_F$ will off-resonantly couple the ancilla's $|g\rangle$ and $|e\rangle$ states, and thus produce a small dynamical phase when the cavities are in other joint photon-number states. To minimize this dynamical effect and to speed up the gate, we successively apply two π pulses to the ancilla: the first one has a duration of 20 ns and is nonselective; while the second one has a duration of 2 μs and involves nine frequency components, each selective on one of the following nine joint Fock states $|j,k\rangle_F$ (j, $k = 0$, 2, 4). With suitable choice of the amplitudes and phases of these driving components, the resulting phase shift associated with the logical state $|22\rangle_F$ differs from those with other joint Fock states by π.

The two-cavity QPT method is also used here to benchmark the realized CZ gate with the binomial encoding, and the measured corresponding Pauli transfer R matrix is displayed in Fig. 4(a). The corresponding process fidelity $F_{\mathrm{CZ\_ED}}$ (F_{ED}) obtained from the measured R matrix is 0.816 (0.922), which indicates the intrinsic CZ gate fidelity $F_{\mathrm{CZ}} = 0.894$. We note that during the gate operation, it is unnecessary to change the photon numbers for both cavities, so that they remain in the original logical space. This gate, together with single-qubit rotations, allows generation of entangled Bell states for the two logical qubits, as shown in Fig. 4(b). We note that single-photon loss can be corrected with this encoding in principle, but the present gate is not realized fault tolerantly as the photon loss occurring during the gate will result in a random phase, destroying the stored quantum information. Recently, fault-tolerant phase gates on single binomially encoded photonic qubit were realized [65,66], however, fault-tolerant implementation of two-qubit gates remains an outstanding task.

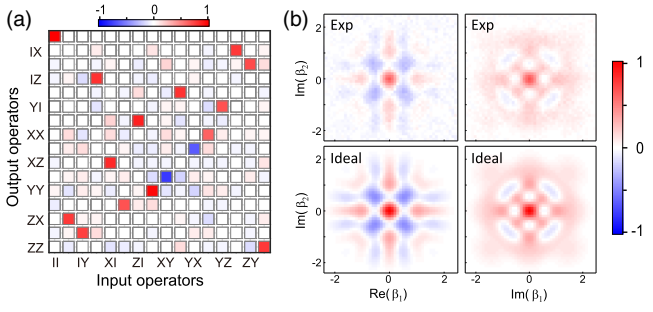

FIG. 4. Two-cavity CZ gate with binomial encoding. (a) Measured Pauli transfer R matrix of the two-cavity CZ gate with the binomial encoding. The corresponding process fidelity $F_{\mathrm{CZ\_ED}}$ (F_{ED}) is 0.816 (0.922). (b) The measured and ideal joint Wigner function of the entangled logical Bell state $|\Phi_+\rangle = (|01\rangle_L + |10\rangle_L)/\sqrt{2}$ on the Im-Re and Im-Im planes, respectively.

Combined with additional single-cavity Hadamard gates of the binomial logical qubits realized by using the GRAPE technique, our two-cavity CZ gate can be used to directly generate an entangled logical Bell state $|\Phi_+\rangle = (|01\rangle_L + |10\rangle_L)/\sqrt{2}$. With the help of two ancillary qubits, joint Wigner tomography of the generated Bell state is performed. The upper row of Fig. 4(b) displays the two slice cuts of the measured two-mode Wigner functions for the generated Bell state, which agree well with those for the ideal logical Bell state shown in the lower row in Fig. 4(b). The fidelity of this entangled state, measured by decoding the logical states back to the ancillary qubits and then performing a joint state tomography, is 0.861.

Besides the controlled-phase gates, the geometric dynamics can be used to realize a two-cavity selective number-dependent arbitrary phase gate [49], which represents an extension of the previously reported selective number-dependent arbitrary phase operation for universal control of a single cavity state [22,23]. The method can also be directly generalized to realize geometric gates among three or more cat-encoded or binomially encoded qubits by properly setting the driving pulse. This kind of gate is useful for quantum error correction [12] and serves as a central element for implementation of the quantum search algorithm [1].

We are grateful for valuable discussions with Chen Wang and Chang-Ling Zou. This work was supported by the National Key Research and Development Program of China No. 2017YFA0304303 and the National Natural Science Foundation of China under Grants No. 11474177, No. 11874114, No. 11674060, No. 11875108, and No. 11874235, and the Natural Science Foundation of Fujian Province under Grant No. 2018J01412.

*These two authors contributed equally to this work.
†zbyang@fzu.edu.cn
‡t96034@fzu.edu.cn
§luyansun@tsinghua.edu.cn

[1] M. A. Nielsen and I. L. Chuang, *Quantum Computation and Quantum Information* (Cambridge University Press, Cambridge, England, 2000), https://doi.org/10.1017/CBO9780511976667.
[2] A. G. Fowler, M. Mariantoni, J. M. Martinis, and A. N. Cleland, Surface codes: Towards practical large-scale quantum computation, Phys. Rev. A **86**, 032324 (2012).
[3] D. G. Cory, M. D. Price, W. Maas, E. Knill, R. Laflamme, W. H. Zurek, T. F. Havel, and S. S. Somaroo, Experimental Quantum Error Correction, Phys. Rev. Lett. **81**, 2152 (1998).
[4] E. Knill, R. Laflamme, R. Martinez, and C. Negrevergne, Benchmarking Quantum Computers: The Five-Qubit Error Correcting Code, Phys. Rev. Lett. **86**, 5811 (2001).
[5] G. Waldherr, Y. Wang, S. Zaiser, M. Jamali, T. Schulte-Herbrüggen, H. Abe, T. Ohshima, J. Isoya, J. F. Du, P. Neumann, and J. Wrachtrup, Quantum error correction in a solid-state hybrid spin register, Nature (London) **506**, 204 (2014).
[6] T. H. Taminiau, J. Cramer, T. van der Sar, V. V. Dobrovitski, and R. Hanson, Universal control and error correction in multi-qubit spin registers in diamond, Nat. Nanotechnol. **9**, 171 (2014).
[7] J. Cramer, N. Kalb, M. A. Rol, B. Hensen, M. S. Blok, M. Markham, D. J. Twitchen, R. Hanson, and T. H. Taminiau, Repeated quantum error correction on a continuously encoded qubit by real-time feedback, Nat. Commun. **7**, 11526 (2016).
[8] X.-C. Yao, T.-X. Wang, H.-Z. Chen, W.-B. Gao, A. G. Fowler, R. Raussendorf, Z.-B. Chen, N.-L. Liu, C.-Y. Lu, Y.-J. Deng, Y.-A. Chen, and J.-W. Pan, Experimental demonstration of topological error correction, Nature (London) **482**, 489 (2012).
[9] J. Chiaverini, D. Leibfried, T. Schaetz, M. D. Barrett, R. B. Blakestad, J. Britton, W. M. Itano, J. D. Jost, E. Knill, C. Langer, R. Ozeri, and D. J. Wineland, Realization of quantum error correction, Nature (London) **432**, 602 (2004).
[10] P. Schindler, J. T. Barreiro, T. Monz, V. Nebendahl, D. Nigg, M. Chwalla, M. Hennrich, and R. Blatt, Experimental repetitive quantum error correction, Science **332**, 1059 (2011).
[11] D. Nigg, M. Müller, E. A. Martinez, P. Schindler, M. Hennrich, T. Monz, M. A. Martin-Delgado, and R. Blatt, Quantum computations on a topologically encoded qubit, Science **345**, 302 (2014).
[12] M. D. Reed, L. DiCarlo, S. E. Nigg, L. Sun, L. Frunzio, S. M. Girvin, and R. J. Schoelkopf, Realization of three-qubit quantum error correction with superconducting circuits, Nature (London) **482**, 382 (2012).
[13] J. Kelly, R. Barends, A. G. Fowler, A. Megrant, E. Jeffrey, T. C. White, D. Sank, J. Y. Mutus, B. Campbell, Y. Chen, Z. Chen, B. Chiaro, A. Dunsworth, I.-C. Hoi, C. Neill, P. J. J. O'Malley, C. Quintana, P. Roushan, A. Vainsencher, J. Wenner, A. N. Cleland, and J. M. Martinis, State preservation by repetitive error detection in a superconducting quantum circuit, Nature (London) **519**, 66 (2015).
[14] A. D. Córcoles, E. Magesan, S. J. Srinivasan, A. W. Cross, M. Steffen, J. M. Gambetta, and J. M. Chow, Demonstration of a quantum error detection code using a square lattice of four superconducting qubits, Nat. Commun. **6**, 6979 (2015).
[15] D. Ristè, S. Poletto, M.-Z. Huang, A. Bruno, V. Vesterinen, O.-P. Saira, and L. DiCarlo, Detecting bit-flip errors in a logical qubit using stabilizer measurements, Nat. Commun. **6**, 6983 (2015).
[16] M. Gong, X. Yuan, S. Wang, Y. Wu, Y. Zhao, C. Zha, S. Li, Z. Zhang, Q. Zhao, Y. Liu, F. Liang, J. Lin, Y. Xu, H. Deng, H. Rong, H. Lu, S. C. Benjamin, C.-Z. Peng, X. Ma, Y.-A. Chen, X. Zhu, and J.-W. Pan, Experimental verification of five-qubit quantum error correction with superconducting qubits, arXiv:1907.04507.
[17] C. K. Law and J. H. Eberly, Arbitrary Control of a Quantum Electromagnetic Field, Phys. Rev. Lett. **76**, 1055 (1996).
[18] A. Ben-Kish, B. DeMarco, V. Meyer, M. Rowe, J. Britton, W. M. Itano, B. M. Jelenković, C. Langer, D. Leibfried, T. Rosenband, and D. J. Wineland, Experimental Demonstration of a Technique to Generate Arbitrary Quantum

Superposition States of a Harmonically Bound Spin-1/2 Particle, Phys. Rev. Lett. **90**, 037902 (2003).
[19] M. Hofheinz, H. Wang, M. Ansmann, R. C. Bialczak, E. Lucero, M. Neeley, A. D. O'Connell, D. Sank, J. Wenner, J. M. Martinis, and A. N. Cleland, Synthesizing arbitrary quantum states in a superconducting resonator, Nature (London) **459**, 546 (2009).
[20] Z. Leghtas, G. Kirchmair, B. Vlastakis, M. H. Devoret, R. J. Schoelkopf, and M. Mirrahimi, Deterministic protocol for mapping a qubit to coherent state superpositions in a cavity, Phys. Rev. A **87**, 042315 (2013).
[21] B. Vlastakis, G. Kirchmair, Z. Leghtas, S. E. Nigg, L. Frunzio, S. M. Girvin, M. Mirrahimi, M. H. Devoret, and R. J. Schoelkopf, Deterministically encoding quantum information using 100-photon Schrödinger cat states, Science **342**, 607 (2013).
[22] S. Krastanov, V. V. Albert, C. Shen, C.-L. Zou, R. W. Heeres, B. Vlastakis, R. J. Schoelkopf, and L. Jiang, Universal control of an oscillator with dispersive coupling to a qubit, Phys. Rev. A **92**, 040303(R) (2015).
[23] R. W. Heeres, B. Vlastakis, E. Holland, S. Krastanov, V. V. Albert, L. Frunzio, L. Jiang, and R. J. Schoelkopf, Cavity State Manipulation Using Photon-Number Selective Phase Gates, Phys. Rev. Lett. **115**, 137002 (2015).
[24] W. Wang, L. Hu, Y. Xu, K. Liu, Y. Ma, S.-B. Zheng, R. Vijay, Y. P. Song, L.-M. Duan, and L. Sun, Converting Quasiclassical States into Arbitrary Fock State Superpositions in a Superconducting Circuit, Phys. Rev. Lett. **118**, 223604 (2017).
[25] Z. Leghtas, G. Kirchmair, B. Vlastakis, R. J. Schoelkopf, M. H. Devoret, and M. Mirrahimi, Hardware-Efficient Autonomous Quantum Memory Protection, Phys. Rev. Lett. **111**, 120501 (2013).
[26] M. Mirrahimi, Z. Leghtas, V. V. Albert, S. Touzard, R. J. Schoelkopf, L. Jiang, and M. H. Devoret, Dynamically protected cat-qubits: A new paradigm for universal quantum computation, New J. Phys. **16**, 045014 (2014).
[27] M. H. Michael, M. Silveri, R. T. Brierley, V. V. Albert, J. Salmilehto, L. Jiang, and S. M. Girvin, New Class of Quantum Error-Correcting Codes for a Bosonic Mode, Phys. Rev. X **6**, 031006 (2016).
[28] N. Ofek, A. Petrenko, R. Heeres, P. Reinhold, Z. Leghtas, B. Vlastakis, Y. Liu, L. Frunzio, S. M. Girvin, L. Jiang, M. Mirrahimi, M. H. Devoret, and R. J. Schoelkopf, Extending the lifetime of a quantum bit with error correction in superconducting circuits, Nature (London) **536**, 441 (2016).
[29] L. Hu, Y. Ma, W. Cai, X. Mu, Y. Xu, W. Wang, Y. Wu, H. Wang, Y. Song, C. Zou, S. M. Girvin, L.-M. Duan, and L. Sun, Quantum error correction and universal gate set on a binomial bosonic logical qubit, Nat. Phys. **15**, 503 (2019).
[30] R. Heeres, P. Reinhold, N. Ofek, L. Frunzio, L. Jiang, M. H. Devoret, and R. J. Schoelkopf, Implementing a universal gate set on a logical qubit encoded in an oscillator, Nat. Commun. **8**, 94 (2017).
[31] S. Rosenblum, Y. Y. Gao, P. Reinhold, C. Wang, C. J. Axline, L. Frunzio, S. M. Girvin, L. Jiang, M. Mirrahimi, M. H. Devoret, and R. J. Schoelkopf, A CNOT gate between multiphoton qubits encoded in two cavities, Nat. Commun. **9**, 652 (2018).
[32] M. V. Berry, Quantal phase factors accompanying adiabatic changes, Proc. R. Soc. A **392**, 45 (1984).
[33] J. Anandan, The geometric phase, Nature (London) **360**, 307 (1992).
[34] F. Wilczek and A. Shapere, *Geometric Phases in Physics* (World Scientific, Singapore, 1989), https://doi.org/10.1142/0613.
[35] S.-B. Zheng, Unconventional geometric quantum phase gates with a cavity QED system, Phys. Rev. A **70**, 052320 (2004).
[36] P. J. Leek, J. M. Fink, A. Blais, R. Bianchetti, M. Göppl, J. M. Gambetta, D. I. Schuster, L. Frunzio, R. J. Schoelkopf, and A. Wallraff, Observation of berry's phase in a solid-state qubit, Science **318**, 1889 (2007).
[37] C. Song, S.-B. Zheng, P. Zhang, K. Xu, L. Zhang, Q. Guo, W. Liu, D. Xu, H. Deng, K. Huang, D. Zheng, X. Zhu, and H. Wang, Continuous-variable geometric phase and its manipulation for quantum computation in a superconducting circuit, Nat. Commun. **8**, 1061 (2017).
[38] A. Wallraff, D. I. Schuster, A. Blais, L. Frunzio, R.-S. Huang, J. Majer, S. Kumar, S. M. Girvin, and R. J. Schoelkopf, Strong coupling of a single photon to a superconducting qubit using circuit quantum electrodynamics, Nature (London) **431**, 162 (2004).
[39] J. Clarke and F. K. Wilhelm, Superconducting quantum bits, Nature (London) **453**, 1031 (2008).
[40] J. Q. You and F. Nori, Atomic physics and quantum optics using superconducting circuits, Nature (London) **474**, 589 (2011).
[41] M. H. Devoret and R. J. Schoelkopf, Superconducting circuits for quantum information: An outlook, Science **339**, 1169 (2013).
[42] X. Gu, A. F. Kockum, A. Miranowicz, Y. X. Liu, and F. Nori, Microwave photonics with superconducting quantum circuits, Phys. Rep. **718–719**, 1 (2017).
[43] H. Paik, D. I. Schuster, L. S. Bishop, G. Kirchmair, G. Catelani, A. P. Sears, B. R. Johnson, M. J. Reagor, L. Frunzio, L. I. Glazman, S. M. Girvin, M. H. Devoret, and R. J. Schoelkopf, Observation of High Coherence in Josephson Junction Qubits Measured in a Three-Dimensional Circuit QED Architecture, Phys. Rev. Lett. **107**, 240501 (2011).
[44] G. Kirchmair, B. Vlastakis, Z. Leghtas, S. E. Nigg, H. Paik, E. Ginossar, M. Mirrahimi, L. Frunzio, S. M. Girvin, and R. J. Schoelkopf, Observation of quantum state collapse and revival due to the single-photon Kerr effect, Nature (London) **495**, 205 (2013).
[45] K. Liu, Y. Xu, W. Wang, S.-B. Zheng, T. Roy, S. Kundu, M. Chand, A. Ranadive, R. Vijay, Y. Song, L. Duan, and L. Sun, A twofold quantum delayed-choice experiment in a superconducting circuit, Sci. Adv. **3**, e1603159 (2017).
[46] Y. Xu, W. Cai, Y. Ma, X. Mu, L. Hu, T. Chen, H. Wang, Y. P. Song, Z.-Y. Xue, Z.-q. Yin, and L. Sun, Single-Loop Realization of Arbitrary Nonadiabatic Holonomic Single-Qubit Quantum Gates in a Superconducting Circuit, Phys. Rev. Lett. **121**, 110501 (2018).
[47] M. Reagor, W. Pfaff, C. Axline, R. W. Heeres, N. Ofek, K. Sliwa, E. Holland, C. Wang, J. Blumoff, K. Chou, M. J. Hatridge, L. Frunzio, M. H. Devoret, L. Jiang, and

R. J. Schoelkopf, Quantum memory with millisecond coherence in circuit QED, Phys. Rev. B **94**, 014506 (2016).
[48] C. Axline, M. Reagor, R. Heeres, P. Reinhold, C. Wang, K. Shain, W. Pfaff, Y. Chu, L. Frunzio, and R. J. Schoelkopf, An architecture for integrating planar and 3D cQED devices, Appl. Phys. Lett. **109**, 042601 (2016).
[49] See Supplemental Material at http://link.aps.org/supplemental/10.1103/PhysRevLett.124.120501 for a discussion of the experimental device and setup, system Hamiltonian, simultaneous readout, encoding and decoding pulses, quantum process tomography, joint Wigner tomography, two-cavity selective number-dependent arbitrary phase gate, and gate error analysis, which includes Refs. [1,21–24,29,43,45–47,50–63].
[50] N. Khaneja, T. Reiss, C. Kehlet, T. Schulte-Herbrüggen, and S. J. Glaser, Optimal control of coupled spin dynamics: Design of NMR pulse sequences by gradient ascent algorithms, J. Magn. Reson. **172**, 296 (2005).
[51] P. de Fouquieres, S. Schirmer, S. Glaser, and I. Kuprov, Second order gradient ascent pulse engineering, J. Magn. Reson. **212**, 412 (2011).
[52] J. M. Chow, J. M. Gambetta, A. D. Córcoles, S. T. Merkel, J. A. Smolin, C. Rigetti, S. Poletto, G. A. Keefe, M. B. Rothwell, J. R. Rozen, M. B. Ketchen, and M. Steffen, Universal Quantum Gate Set Approaching Fault-Tolerant Thresholds with Superconducting Qubits, Phys. Rev. Lett. **109**, 060501 (2012).
[53] C. Wang, Y. Y. Gao, P. Reinhold, R. W. Heeres, N. Ofek, K. Chou, C. Axline, M. Reagor, J. Blumoff, K. M. Sliwa, L. Frunzio, S. M. Girvin, L. Jiang, M. Mirrahimi, M. H. Devoret, and R. J. Schoelkopf, A Schrödinger cat living in two boxes, Science **352**, 1087 (2016).
[54] Y. Y. Gao, B. J. Lester, K. S. Chou, L. Frunzio, M. H. Devoret, L. Jiang, S. M. Girvin, and R. J. Schoelkopf, Entanglement of bosonic modes through an engineered exchange interaction, Nature (London) **566**, 509 (2019).
[55] M. Reagor, H. Paik, G. Catelani, L. Sun, C. Axline, E. Holland, I. M. Pop, N. A. Masluk, T. Brecht, L. Frunzio, M. H. Devoret, L. Glazman, and R. J. Schoelkopf, Reaching 10 ms single photon lifetimes for superconducting aluminum cavities, Appl. Phys. Lett. **102**, 192604 (2013).
[56] F. Motzoi, J. M. Gambetta, P. Rebentrost, and F. K. Wilhelm, Simple Pulses for Elimination of Leakage in Weakly Nonlinear Qubits, Phys. Rev. Lett. **103**, 110501 (2009).
[57] J. M. Gambetta, F. Motzoi, S. T. Merkel, and F. K. Wilhelm, Analytic control methods for high-fidelity unitary operations in a weakly nonlinear oscillator, Phys. Rev. A **83**, 012308 (2011).
[58] E. Knill, D. Leibfried, R. Reichle, J. Britton, R. B. Blakestad, J. D. Jost, C. Langer, R. Ozeri, S. Seidelin, and D. J. Wineland, Randomized benchmarking of quantum gates, Phys. Rev. A **77**, 012307 (2008).
[59] J. M. Chow, J. M. Gambetta, L. Tornberg, J. Koch, L. S. Bishop, A. A. Houck, B. R. Johnson, L. Frunzio, S. M. Girvin, and R. J. Schoelkopf, Randomized Benchmarking and Process Tomography for Gate Errors in a Solid-State Qubit, Phys. Rev. Lett. **102**, 090502 (2009).
[60] E. Magesan, J. M. Gambetta, B. R. Johnson, C. A. Ryan, J. M. Chow, S. T. Merkel, M. P. da Silva, G. A. Keefe, M. B. Rothwell, T. A. Ohki, M. B. Ketchen, and M. Steffen, Efficient Measurement of Quantum Gate Error by Interleaved Randomized Benchmarking, Phys. Rev. Lett. **109**, 080505 (2012).
[61] E. Magesan, J. M. Gambetta, and J. Emerson, Scalable and Robust Randomized Benchmarking of Quantum Processes, Phys. Rev. Lett. **106**, 180504 (2011).
[62] R. Barends, J. Kelly, A. Megrant, A. Veitia, D. Sank, E. Jeffrey, T. C. White, J. Mutus, A. G. Fowler, B. Campbell, Y. Chen, Z. Chen, B. Chiaro, A. Dunsworth, C. Neill, P. O'Malley, P. Roushan, A. Vainsencher, J. Wenner, A. N. Korotkov, A. N. Cleland, and J. M. Martinis, Superconducting quantum circuits at the surface code threshold for fault tolerance, Nature (London) **508**, 500 (2014).
[63] D. F. V. James, P. G. Kwiat, W. J. Munro, and A. G. White, Measurement of qubits, Phys. Rev. A **64**, 052312 (2001).
[64] L. Sun, A. Petrenko, Z. Leghtas, B. Vlastakis, G. Kirchmair, K. M. Sliwa, A. Narla, M. Hatridge, S. Shankar, J. Blumoff, L. Frunzio, M. Mirrahimi, M. H. Devoret, and R. J. Schoelkopf, Tracking photon jumps with repeated quantum nondemolition parity measurements, Nature (London) **511**, 444 (2014).
[65] P. Reinhold, S. Rosenblum, W.-L. Ma, L. Frunzio, L. Jiang, and R. J. Schoelkopf, Error-corrected gates on an encoded qubit, arXiv:1907.12327.
[66] Y. Ma, Y. Xu, X. Mu, W. Cai, L. Hu, W. Wang, X. Pan, H. Wang, Y. P. Song, C. L. Zou, and L. Sun, Error-transparent operations on a logical qubit protected by quantum error correction, arXiv:1909.06803.